

Matter, Volume 3

Supplemental Information

**Reducing False Negatives
in COVID-19 Testing by Using
Microneedle-Based Oropharyngeal Swabs**

Wei Chen, Bo Cai, Zhi Geng, Fenghua Chen, Zheng Wang, Lin Wang, and Xiaoyuan Chen

Supplemental data items

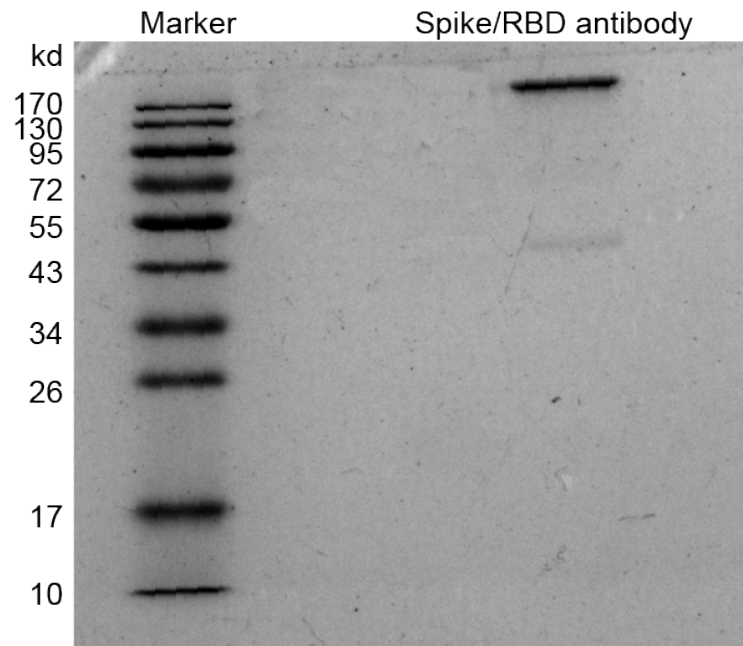


Figure S1. Sodium dodecyl sulfate polyacrylamide gel electrophoresis (SDS-PAGE) analysis of Spike/ RBD antibody. The data indicates the purity of the antibody released from MN patches, demonstrating the stability of the antibody during integration into the patches.

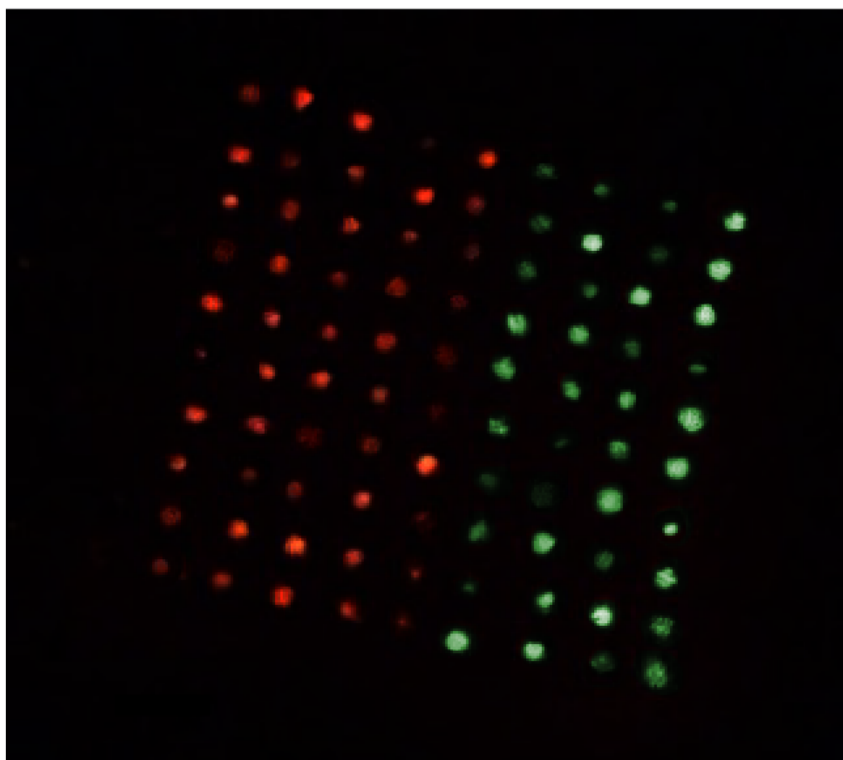


Figure S2. Fluorescence distribution of the dually functionalized MN patch containing rhodamine and FITC. It should be mentioned that as the two patches were fabricated and then combined together, it is easy to adjust the ratio of differentially functionalized MNs. Moreover, the payload in each patch could be completely separated without any overlap, indicating a precise control of the payload distribution.

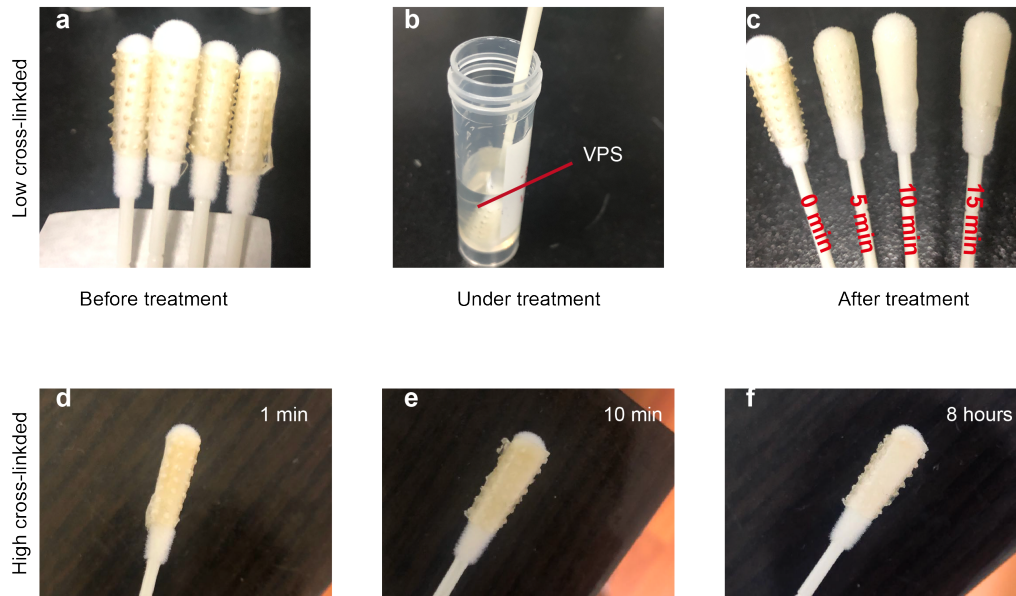


Figure S3. Dissolving behavior of low and high cross-linked MNs. (a-c) For low cross-linked patches, they would rapidly and readily dissolve in virus preservation solution (VPS) within 15 minutes. (d-f) High cross-linked patches could act as a stable species in VPS for at least 8 hours. The different dissolving behaviors of patches provided both capabilities of tissue penetration and virus collection, as well as the subsequent virus release.

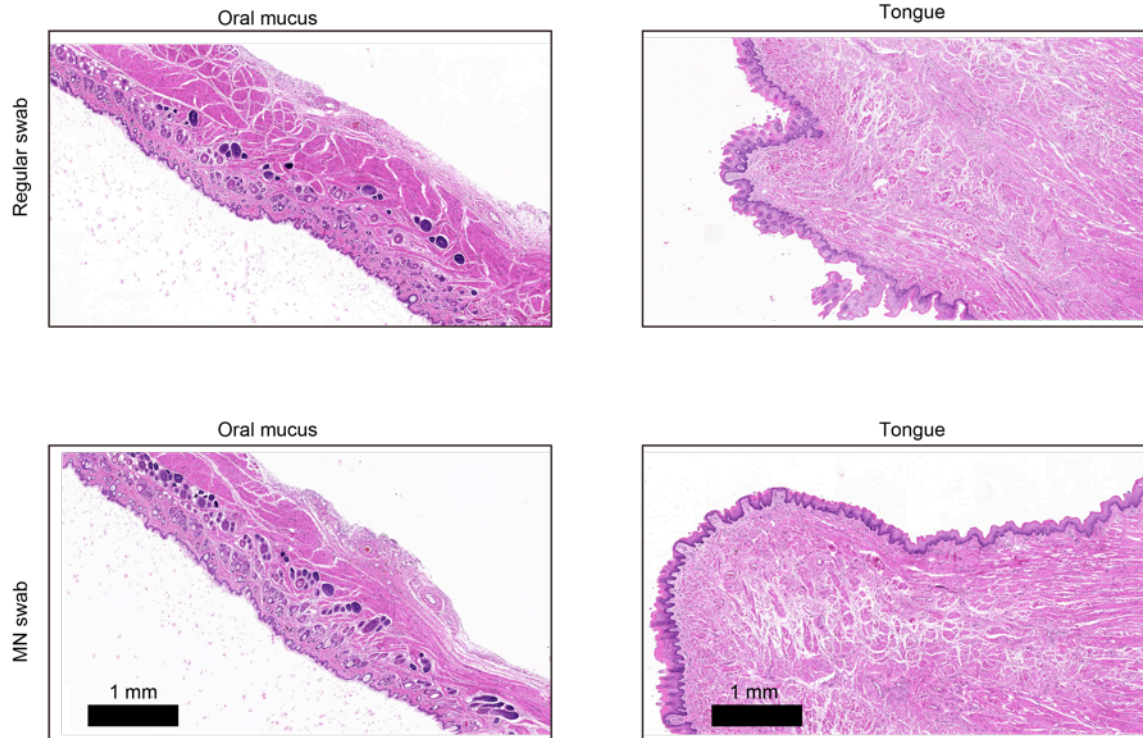


Figure S4. Histology analysis of oral mucus and tongue after treatment by regular and MN swabs. After treatment (24 h later), samples from oral mucus and the tongues were analyzed using haemotoxylin and eosin (H&E) staining. Importantly, no obvious injuries were found after regular or MN swab treatments. Considering some micro-channels were observed immediately after MN swab treatment, this staining result suggests that the channels could be spontaneously recovered within one day.

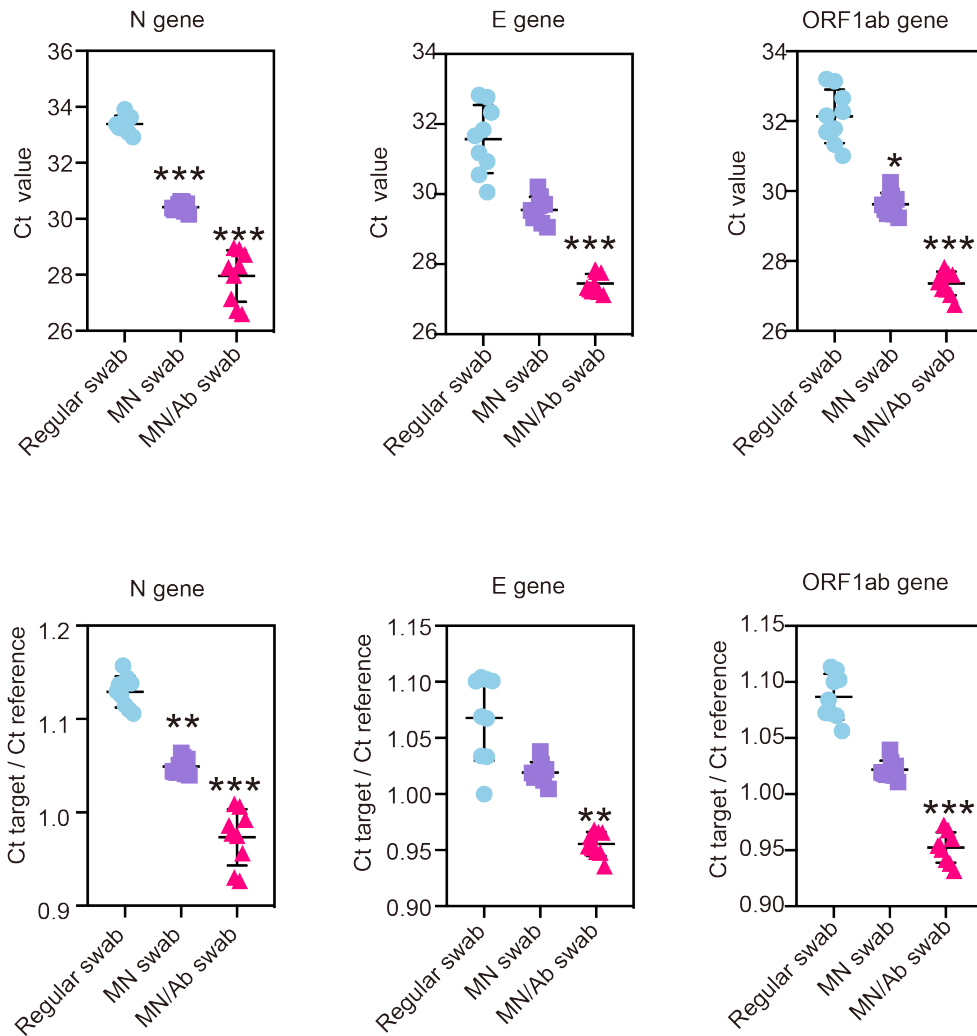


Figure S5. Comparisons of sampling efficiency of different swabs in the rat model. All three genes indicated that MN/Ab swab showed an obvious sampling enhancement compared to others no matter in absolute Ct values or relative Ct values. Mean \pm SD (n = 9). *P < 0.05, **P < 0.01, ***P < 0.001.

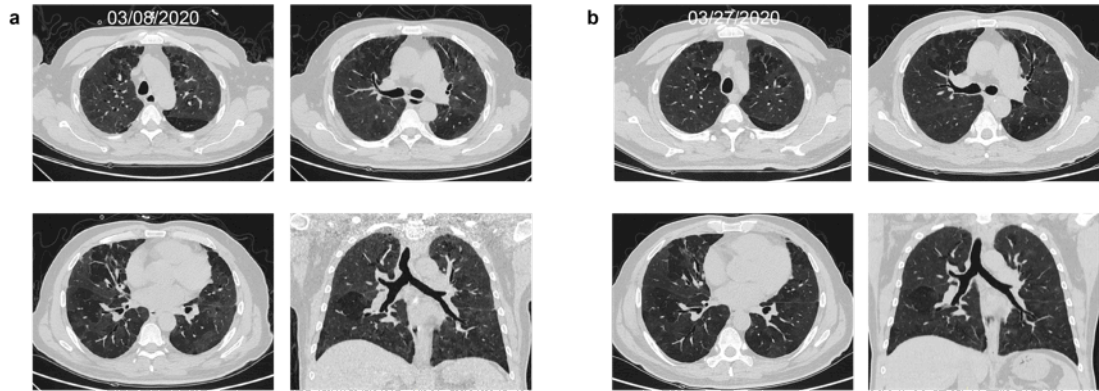
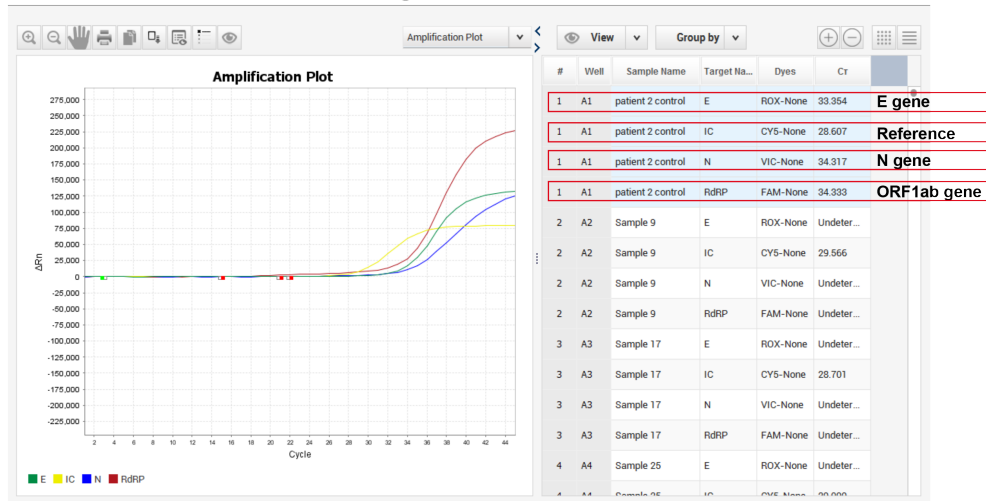


Figure S6. CT imaging characteristics of a COVID-19 positive patient. (a and b) Ground-glass opacity and consolidation were clearly detected at different time points. The sampling with the MN/Ab swabs took place in the first week of hospitalization. After early diagnosis as COVID-19, the patient was isolated and has completely recovered.

Positive patient

Regular swab



MN/Ab swab

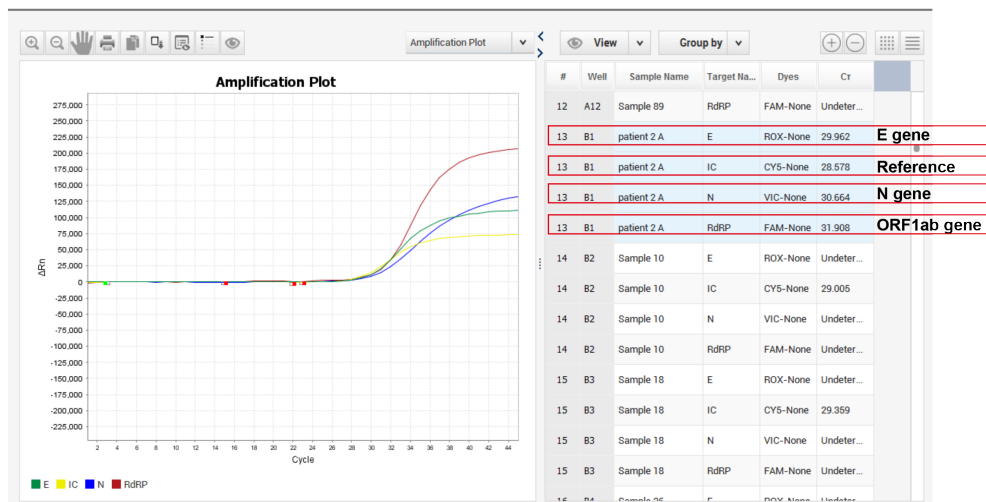
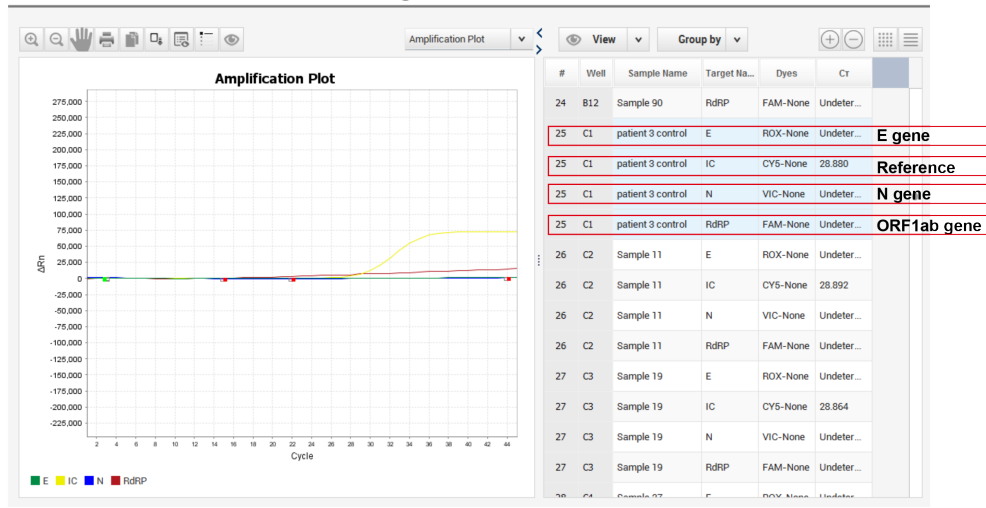


Figure S7. qRT-PCR results of regular and MN swabs for a positive patient. Obviously, MN/Ab swab treatment induced lower Ct values compared to regular ones, suggesting a higher sampling efficiency.

Negative patient

Regular swab



MN/Ab swab

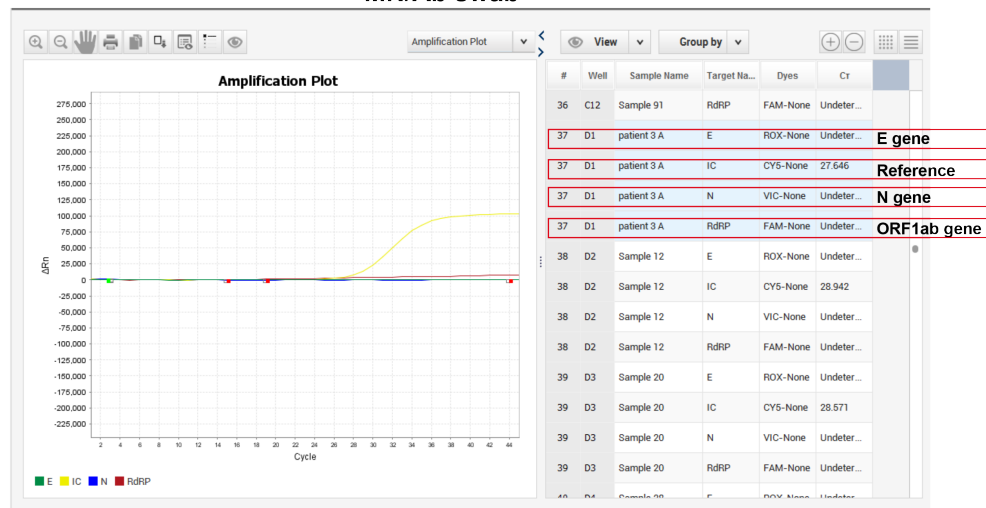


Figure S8. qRT-PCR results of regular and MN/Ab swabs for a negative patient. After measuring the samples from negative patients, only internal reference shows detectable signals while ORF1ab gene, N gene and E gene presented negative signals, indicating that no false positives were observed for both swabs. This demonstrates that the MN/Ab swab testing can be a feasible and reliable detection approach.